



EGYPTIAN ACADEMIC JOURNAL OF

BIOLOGICAL SCIENCES

MEDICAL ENTOMOLOGY & PARASITOLOGY

E



ISSN
2090-0783

WWW.EAJBS.EG.NET

Vol. 14 No. 2 (2022)



Prevalence and Morphological Characterization of the Camel Nasal Botfly, *Cephalopina titillator* (Diptera: Oestridae) Collected from Abattoirs in Egypt

Sherif Hamed, Mona G. Shaalan, Emad I. Khater, Mohamed A. Kenawy and Enas H. Ghallab*

Entomology Department, Faculty of Science, Ain Shams University, Cairo, Egypt.

E-mail : enashamdy@sci.asu.edu.eg

ARTICLE INFO

Article History

Received:28/8/2022

Accepted:18/10/2022

Available:21/10/2022

Keywords:

Camel nasal botfly,
Cephalopina titillator,
Oestrid flies,
prevalence, myiasis,
Egypt

ABSTRACT

The Arabian camel (*Camelus dromedarius*) is considered one of the important livestock that has a major impact on humans' life, especially economically. Larval stages of the camel nasal botfly, *Cephalopina titillator* (Diptera: Oestridae), come on the top list of obligate endoparasites causing nasopharyngeal myiasis leading to huge economic loss to the camel culture and industry all over the world. Although adult flies are not parasitic and are unable to feed, they can survive on the nutrient reserve from the larval stages. In Egypt, little is known about the biology and ecology of *C. titillator* and the role of the ambient ecological factors in affecting larval development as associated with the camel host and under laboratory conditions. To address this knowledge gap, we studied morphology, population structure, and seasonal prevalence of *C. titillator* larval stages in camels in Egypt. A total of 429 of both 2nd and 3rd stage larvae were collected from slaughtered camel's heads in El-Bassatin abattoir over a 12-months period, from June 2019 to May 2020. Out of the 62 examined animal heads, 33 (53.23%) were infested. The mature 3rd instar larvae were reared in the laboratory at different ambient temperatures and observed till the emergence of the adult stages. Detailed morphological characterization and fine ultrastructure for both the larval instars and adult flies are provided using light and scanning electron microscopic examination, respectively. Therefore, this study showed the importance of body characteristics that are among the important dimorphic features of adult flies.

INTRODUCTION

The one-humped camel or the Arabian camel, *Camelus dromedarius*, occupies economic and cultural importance in the Arabian communities, where they adapted to the harsh conditions of the arid and semiarid regions. The camel industry mainly relies on camels for milk, meat, and skin, and for trade, transport, and sports racing means both in nomadic communities and modern societies. However, camels' livestock suffers from several parasitic agents that cause diseases and therefore, reduce their health, well-being, quality of meat and other products. (Abd El-Rahman 2010). The camel nasal botfly, *Cephalopina titillator*, is a common obligate endoparasite of both camel females and males, causing myiasis as a result of animal infestation and feeding by fly larval stages.

Although there is no clear study that illustrates the worldwide distribution of *C. titillator* flies, their geographic distribution is determined by the presence of their animal hosts wherever they are found. The Middle East region, Africa and India are the commonly known homes for the Arabian camel wealth due to their environmental nature of arid and semi-arid habitats suitable for camel life, with its associated ecto-/endo-parasites (Locklear *et al.*, 2021).

Camel infestation with camel nasal botflies was reported in Egypt (Morsy *et al.*, 1998, Khater *et al.*, 2013), Saudi Arabia (Hussein *et al.*, 1982, Fatani and Hilali 1994, Alahmed 2002), Libya (Abd El-Rahman 2010), Jordan (Al-Ani and Amr 2016), Iraq (Al-Jindeel *et al.* 2018), Sudan (Musa *et al.*, 1989), Iran (Jalali *et al.*, 2016, Oryan *et al.*, 2008), Nigeria (Desbordes and Ajogi 1993) and Ethiopia (Bekele 2001, Kissi and Assen 2018). In China, it was also reported that *Camelus bactrianus* (Bactrian camel) was infested with nasal botflies of the same species (Li *et al.*, 2020).

Camel nasal botflies are specialized in the nasopharyngeal myiasis resulting in host breathing difficulties, pathological lesions in tissues and severe irritation leading to loss of appetite, retardation in milk production, loss of weight and meat quality, and eventual animal death from meningitis caused by secondary infections, with overall significant veterinary and economic losses (Fatani and Hilali 1994, Otranto 2001, Oryan *et al.*, 2008, Jalali *et al.*, 2016).

Such fly-infestation-caused myiasis imposes a negative health state on the infested camels. Clinical diagnosis reveals characteristic symptoms such as nasal discharges that causes difficulty in breathing accompanied by frequent snorting which is the common theme of such infestation. The severe infestation leads to blockage of the nasopharyngeal passage by both the larvae and the induced mucus secretion. The camel infestation by *C. titillator* might lead to an alternation in the thyroid-pituitary function causing hypothyroidism status (El-Bassiony *et al.*, 2005).

Cephalopina titillator life cycle starts when the non-parasitic and non-feeding female fly darts the first larval instars towards the base of camel nostrils. Larvae migrate towards the nasopharyngeal passage, invading its sinuses and pouches up to the pharyngeal diverticula aided by their body spinulation in addition to their

mouth hooks, which play a pivotal role in larval attachment and movement. Developmental periods for the fly's first larval instars significantly vary, ranging from days to months. It is reported that even larvae ejected from the same female fly may have a different rate of development. Although the development regulating factors are not well-studied, it is suggested that fly species and population structure, larval crowding, host immunity and climatic conditions may have a role in the onset of hypnosis (i.e., phases of arrested development) (Colwell 2006, Angulo-Valadez *et al.*, 2010).

During the migratory route, the larvae pass through two moults giving the second and third instars. Once they have reached larval maturity, the usual leaving strategy is through the host's sneezing behaviour to relieve the irritation in the nasal passage. Subsequently, the larvae fall onto the ground in the vicinity of the host. Due to the parasite's negative phototropic behaviour, they seek a shaded sandy substrate to burrow into to evade the harsh environmental conditions outside the host body (Ruiz-Martines and Palomares 1993).

The aim of this study was to investigate the population structure, seasonal prevalence, and infestation rate of the second and third instars larvae of *C. titillator* infesting camels in Egypt. We aimed also at providing descriptive morphologic and fine structure descriptions for taxonomic studies of the collected larvae and reared adult flies of both sexes.

MATERIALS AND METHODS

Sample Collection Area:

This study was conducted at EL-Bassatin abattoir situated in Cairo Governate, Egypt (29.995917N, 31.276171E). It is considered one of the largest and most commonly used abattoirs that are responsible for slaughtering camels in Egypt.

Study Animals:

This study was done on 62 camels slaughtered in El-Bassatin abattoir. Most of

the camels examined have been brought from Sudan. The slaughtered camels were more than three years of age.

Sample Collection and Identification of Larvae:

Different stages of *C. titillator* larvae were monthly collected from infested camel's heads from June 2019 to May 2020. Heads of slaughtered camels were separated from the rest of the body and the skull was incised sagittally or coronally through the throat until reaching the nasopharynx. The Skull incision process was made by the slaughter's butchers under the supervision of veterinarians. Nasal and pharyngeal cavities were examined for the presence of larvae. The obtained larvae were collected in sterilized plastic cups labelled with the date of collection and transferred to the Department of Entomology laboratory at the Faculty of Science, Ain Shams University for further processing and studies. In the laboratory, the live larvae were washed with tap water to eliminate any remnant camel mucus and secretions.

After differentiation into 2nd and 3rd larval instars according to Zumpt (1965), the larvae were preserved in 70% ethyl alcohol for detailed morphological identification (Schauff 2001). It was difficult to identify the 1st instar larvae due to their tiny size (0.7 mm) and camel slaughtering circumstances (Zumpt 1965, Hussein *et al.*, 1982, Fatani and Hilali 1994, Oryan *et al.*, 2008). A special group of mixed larvae was collected by the butcher's assistance and contained a bunch of larvae from several heads in a large sterilized jar. This group from which we chose the highly active 3rd instar larvae to be reared to the adult stage.

Rearing of the Collected 3rd Instar Larvae to The Adult Stage:

The completely matured and active 3rd instar larvae were placed in a plastic container. The container was half-filled with moisturized sterilized sand and placed in an insect-rearing box (Fahmy *et al.*, 1985, Bekele 2001). The rearing process was made under room conditions to mimic the

natural environmental conditions of the fly and host habitat in the insectary of Entomology Department, Faculty of Science, Ain Shams University. Throughout the rearing period, both temperature and humidity were recorded daily. The larval rearing process was repeated three times over three different seasons (Summer, Autumn and Winter) during which the reared larvae were daily observed till adult emergence. For Spring season (March, April & May, 2020) coincided with the summit of Covid 19 pandemic and also there were great restrictions in the slaughterhouse for collecting large number of samples for rearing. Each emerging adult was kept in a separate vial marked with the day of emergence.

Morphological and Ultrastructure Examination:

A- General Fly Morphology Examination by Light Stereomicroscope:

General fly morphology was inspected using an Optika stereoscopic microscope (OPTIKA Corp., Ponteranica, Italy). The larvae identification and body measurements for classification were performed according to Zumpt (1965). The cephalic region with the mouth-hooks, antennal lobes, body spinulation, the thoracic and abdominal region with spines and posterior peritremes (plate that surrounds the spiracles in some insects) were all examined for both 2nd and 3rd instars. Adult flies overall colour of the body, the separation of eyes in the head region, the shape of the frons and the antennal groove with the antennal structure, the thoracic region and the shape of the wing in respect to the venation distribution and the abdominal structure were examined. Mouth hooks, spiracular plates of both larval instars and the legs of the adult flies were slide-mounted on glycerine using flat slides. The image handling and plate formation were processed using Adobe Photoshop CS6 (Adobe Systems, Inc., San Jose, CA, USA) on Windows 10 platform (Li *et al.*, 2018). The scale bar on each

image was added using ImajeJ software (version 1.53k, 2021) using the original body measurement of the sample (Schneider *et al.*, 2012).

B- Fly ultrastructure examination with scanning electron microscopy:

Preparations for **ultrastructure examination** were made on freshly collected second and third larval instars. After washing several times with tap water, they were immediately immersed in 2.5% glutaraldehyde for fixation and storage (Hilali *et al.*, 2015). Large-size specimens, especially in the late third instar, were sectioned with a sharp scalpel blade into three parts. Horizontal cuts separating the anterior four segments and the posterior three segments from the mid-portion of each specimen and internal organs were removed (Colwell 1998, El-Bassiony and Awad 2007).

Specimens were passed through a series of ascending concentrations (50%, 70%, 90%, and 100%) of ethyl alcohol for dehydration and dried in CO₂ critical point

RESULTS

A total of 62 camel heads were separated from the rest of the body and the skull was incised sagittally or coronally through the throat until reaching the

drier (Autosamdri-815, Germany). The dried specimen sections were then glued over metal stubs and covered with 20 nm gold in a sputter coater (Spi-Module sputter Coater, UK). Eventually, specimens were examined and photographed with a scanning electron microscope (JSM 5200, Electron Prob Microanalyzer, Jeol, Japan) at the Faculty of Agriculture, Cairo University, according to the method described (Hilali *et al.*, 2015).

Statistical Analysis:

Data generated from post-mortem examination for both larval and adult stages accompanied with the recorded weather data were stored in the Microsoft Excel sheets. Data were statistically analysed using the statistical analysis and visualization R programming language for statistical computing version (4.1.0) (Hartvigsen 2014). Pearson's correlation coefficient (r) test was performed to evaluate the association between the studied variables. The *P* value of less than 0.05 was considered significant.

nasopharynx (Fig. 1). examination of camel heads over the 12-months study period showed that 33 (53.23%) camels have been infested with *C. titillator* at different larval stages (Table 1).



Fig. 1: Camel's head that was cut sagittally (A&B) and coronally (C) through the throat (by the slaughter's butchers under veterinarians' supervision) until reaching the nasopharynx showing a number of crawling larvae.

Table 1: The monthly prevalence of *C. titillator* larvae infestation among camels in El-Bassatin abattoir, Cairo, Egypt, from June,2019 to May,2020.

Date of slaughtering	No. of Examined camels	No. of Infected camels	**Rate of camel infestation (%)	No. of infected larvae				Total		Temperature
				Second Instar		Third Instar		No.	Index	
				No.	Index*	No.	Index			
18 th June,2019	7	2	28.6%	4	2	15	7.5	19	9.5	36°C
16 th July,2019	5	1	20%	3	3	8	8	11	11	39°C
20 th Aug,2019	5	2	40%	7	3.5	11	5.5	18	9	34°C
17 th Sept,2019	5	2	40%	12	6	19	9.5	31	15.5	33 °C
15 th Oct,2019	5	3	60%	17	5.6	23	7.7	40	13.3	31 °C
19 th Nov,2019	5	4	80%	14	3.5	35	8.8	49	12.2	25 °C
24 th Dec,2019	5	4	80%	18	4.5	48	12	66	16.5	19 °C
14 th Jan,2020	5	3	60%	15	5	34	11.3	49	16.3	18 °C
11 th Feb,2020	5	4	80%	12	3	44	11	56	14	18 °C
17 th Mar,2020	5	3	60%	9	3	31	10.3	40	13.3	18 °C
14 th April,2020	5	3	60%	5	1.6	29	9.6	34	11.3	26 °C
12 th May,2020	5	2	40%	3	1.5	13	6.5	16	8	34 °C
Total	62	33	53.23 %	119	3.60	310	9.39	429	13	

* Larval index = number of larvae/infected animal

** Rate of camel infestation (%) = (# of infested camels / Total # of examined camels) ×100

The total number of all larval instars in each month is shown in Table (1). The results showed that the highest camel infestation rate (80%) was recorded in November and December 2019 and February 2020. This was followed by October 2019 January, and March, and April 2020 with 60%. The lowest infestation rate (20%) was recorded in July 2019. Hence, the relationship between the

infestation rate and the collection month was following the normal distribution using the Shapiro-Wilk test (p -value= 0.2) (Fig. 2). In addition, the relationship between ambient temperature and the rate of infestation we need to delete (and) before ambient and ambient temperature and the rate of infestation was estimated through Pearson's correlation test ($r = -0.85$, $P = 0.0005$) (Fig. 3).

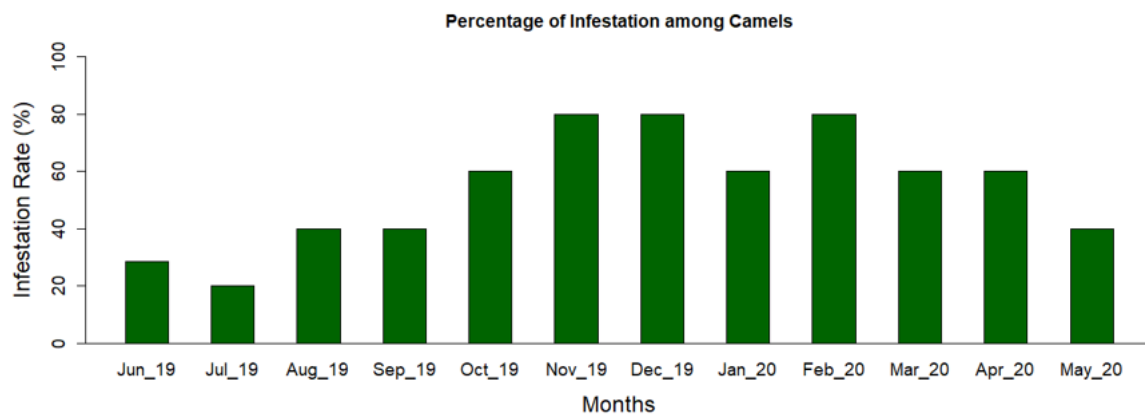


Fig. 2: Histogram represents the percentage of infestation among camels with *Cephalopina titillator* throughout a year.

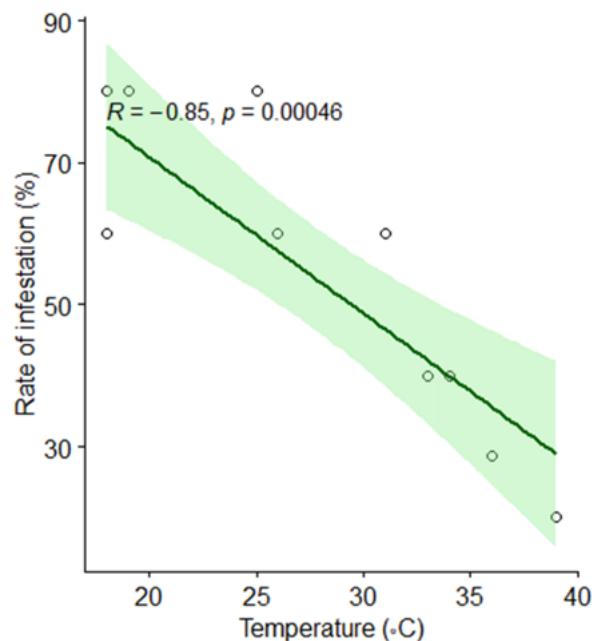


Fig. 3: Relationship between infestation rate and temperature revealing strong negative correlation.

The total number of all larval instars per camel per month (larval index) was estimated. The highest larval indices were estimated at (16.5) and (16.3) in December 2019 and January 2020, respectively, while the lowest index (8) was observed in May 2020. The second instars index reached its peak (6) in September 2019, whereas the lowest index (3.5) was observed in November 2019. Furthermore, the third larval instars showed high abundance from December 2019 (12) to February 2020 (11) with nearly a steady rate, but unlike the second instars, the third instar's lowest index (5.5) was in August 2019.

For each season, the rate of camel infestation was calculated (Table 2). The highest infestation rate (73.3%) occurred in the winter season, while the lowest rate (29.41%) was in the summer season. The estimated larval index for both the third and second instar larvae reached 15.54 in the winter season followed by the autumn season (13.3) then the spring season (11.25) and finally the summer season (9.6). In addition, the larval index and the percentage for each instar were calculated separately for the different seasons (Figs. 4&5).

Table 2: The seasonal prevalence of *C. titillator* larvae infestation among camels in El-Bassatin abattoir, Cairo, Egypt, from June 2019 to May 2020.

Season of collection	No. of Examined camels	No. of Infected camels	Rate of infestation	infected larvae				Total	
				Second Instar		Third Instar		No.	Index
				No.	Index	No.	Index		
Summer (June, July and Aug)	17	5	29.41%	14	2.8	34	6.8	48	9.6
Autumn (Sept, Oct and Nov)	15	9	60%	43	4.78	77	8.55	120	13.3
Winter (Dec, Jan and Feb)	15	11	73.3%	45	4.09	126	11.45	171	15.54
Spring (Mar, April and May)	15	8	53.3%	17	2.12	73	9.12	90	11.25

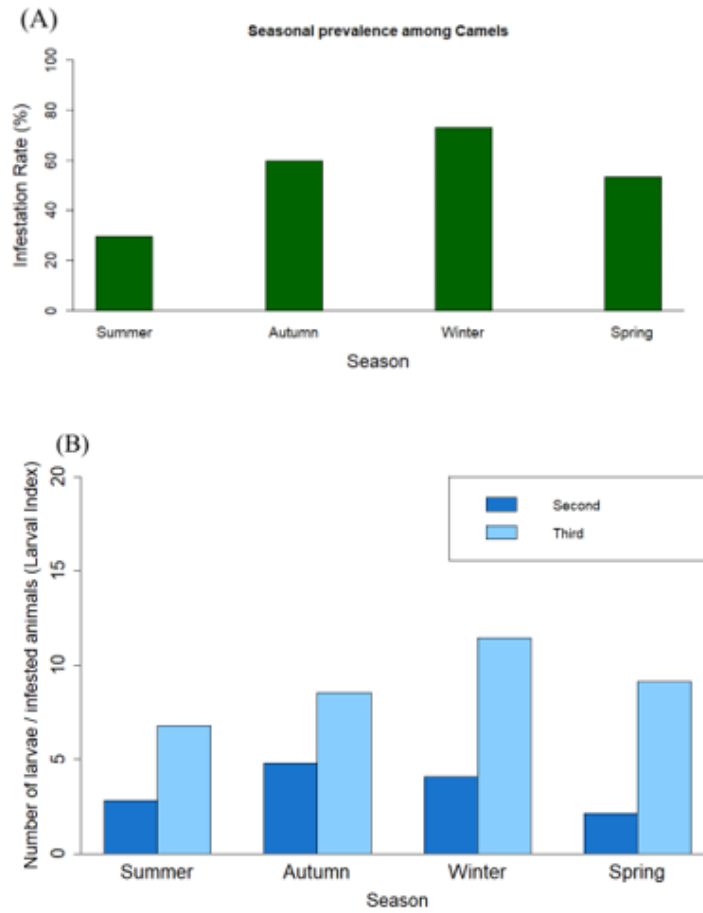


Fig. 4: Histogram represents the seasonal variation of camel infestation with *Cephelopina titillator*. **(A)** Seasonal prevalence among camels and **(B)** the larval index for each season. (Larval index = number of larvae/number of infected animals).

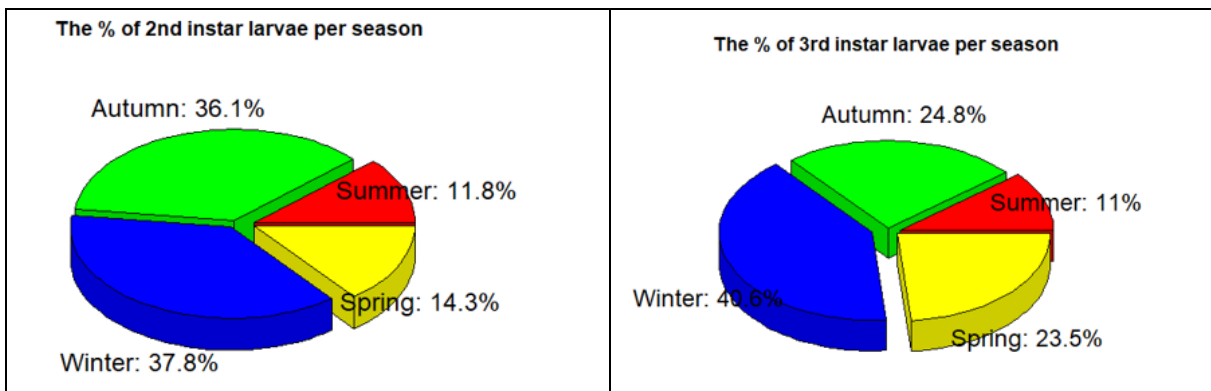


Fig. 5: Pie charts showing the percentage of *Cephelopina titillator* larval infestation of camels for each instar separately in relation to the different seasons.

Rearing of the Collected *C. titillator* Third Instar Larvae:

On the first day, it was noticeable the vigorous burrowing activity in the sand. This vigorous movement lasted for the second day where some dipped themselves in the sand while the rest remained on the

surface. On the third day, there were very slow movements for the group that stayed on the surface accompanied by a slight darkening in colour.

The collected *C. titillator* third instar larvae were reared in three different periods representing different weather conditions.

The first was performed in August 2019 as a representative for the summer season. Out of 42 larvae, only five adult flies have emerged. The first male fly emerged on the 13th day of pupation, while the second and the third adults emerged as male and female flies, respectively on the 19th day, the fourth female emerged on the early morning of the 21st day, and it took 22 days for the fifth female fly to emerge since pupation (Table 3).

The second round of rearing was performed in November 2019 as a representative for the Autumn season. Out of 38 collected third instar larvae, only three

adults have emerged. The first fly emerged as a male on its 17th day of pupation, followed by the second fly on day 23rd as a female, while the last fly emerged as a female on the 28th day of pupation. The inspection was continued for further two weeks for any new adult emergences.

For the third rearing trial which occurred in February 2020 as a representative for the Winter season, there were no adult flies that emerged out of 31 collected larvae. The cages were daily inspected for more than six weeks but they showed no emergence.

Table 3: Rearing of third instar larvae under room conditions showing the adult emergence rate in different environmental conditions.

Date of slaughtering	No. of larvae	No. of emerged adults	Sex		**Rate of emergence	*Temperature		*Humidity	Pupation period (Days)
			Male	Female		Min.	Max.		
20th Aug, 2019	42	5	2	3	12%	25°C	34°C	36%	13 - 22
19th Nov, 2019	38	3	1	2	7%	14°C	25 °C	16%	17- 28
11th Feb, 2020	31	0	-	-	-	9°C	18°C	51%	-

Morphological examination:

The morphological characters of the 2nd and 3rd larval instars of *C. titillator* were investigated using light and scanning electron microscopes. Second instar larvae were dorsoventrally flattened, slender in shape with a rounded dorsal surface (Fig. 6A&B). Body composition follows the normal larval stereotype of having 12 segments (one cephalic, three thoracic, and eight abdominal) with a mean body length and width of 12.59 ± 2.108 mm and 3.416 ± 0.37 mm, respectively. The Head region (pseudocephalon) is characterized by widely separated antennal lobes, well-developed obligate mouth hooks (maxillae), about 2/3 the length of pseudocephalon height (Fig. 6C). Hidden sickle-like cephalic hooks (mandibles) appear from the larval cuticle in the head region are also observed (Fig. 6C&D).

Dorsally, with the exception of the thoracic regions, there are no spines

throughout the abdomen (Fig. 6A). Regarding the instar spinulation, spines are very tiny and obvious on the ventral surface, especially the thoracic segments and gradually decrease toward the end of the abdomen (Fig. 6B). Scanning Electron Microscope revealed the presence of cuticular pits and inter-segmental grooves (Fig. 7A&B). The magnified antennal lobes are devoid of the pseudocelli which appear in the latter instars (Fig. 7C). The spiracular preitremes on the last abdominal segment are oval-shaped, hidden in a sunken groove, and surrounded by spiny lips. Preitremes' pores appear in a sickle shape or the falciform structure counted to range from (9 -12) pores (Fig. 6E&F, 7D&E).

The third instar larvae were dorsoventrally flattened with a mean body length and width (\pm S.E.) of 22.80 ± 3.07 mm and 8.30 ± 0.7 mm, respectively. Dorsally, the body is provided with a few cuticular pits; the anterior part of the body

is armed with rows of irregular spines decreasing in number gradually till disappearing in the 7th and 8th abdominal segments (Fig. 8A & B). There are clear rows of tiny spines located just behind the fleshy processes in an alternative manner throughout the body segments, however, the spine rows were interrupted on the lateral side. These rows become denser and clearer on the anteroventral side of the thoracic segments taking an irregular distribution while their number decrease in the subsequent postero-ventral abdominal segments (Fig. 8 C & D). The latero-posterior side of the 1st thoracic segment bears a pair of anterior spiracles; in addition to 17 smooth and fleshy processes on the body segments, eight of them are located ventrally and nine dorsally. The pseudocephalon is occupied with apparently large, ventrally curved and sharply pointed cephalic hooks, maxillae, surrounding the atrium; two broadly separated antennal lobes (Fig. 8E). The structure of the cephalopharyngeal skeleton was separated from the body and dissected to expose its fine details of the oral hooks and the hypostomal sclerites (Fig. 8F). At

the terminal part of the body, the lower and upper lips surrounding the posterior spiracles provided with very dense spines (Fig. 8G). Posterior spiracles are kidney-shaped, surrounding but not enclosing a stigma (ecdysal scare), with numerous irregular oval-to-kidney shaped pores with a mean length and width of 1.22 ± 0.038 mm and 0.788 ± 0.003 mm, respectively (Fig. 8H).

The detailed view of the third instar using SEM showed that the cephalic hooks are smooth and non-ornamented (Fig. 9 A & B). The antennal lobes are widely separated and occupied with well-developed pseudo-ocelli that is deterministic of the mature 3rd stage only (Fig. 9C). The magnification of body details showed the presence of large inward grooves between the thoracic segments accompanied by conspicuous cuticular pits, each is encircled by cuticular wrinkles in the 2nd and 3rd thoracic segment (Fig. 9 D & E). Lips on the last abdominal segment show the spiracular peritremes and the anal orifice on the anal papillae (Fig. 9F), in addition to eight sensory tubercles, four on each lip (Fig. 9G & H).

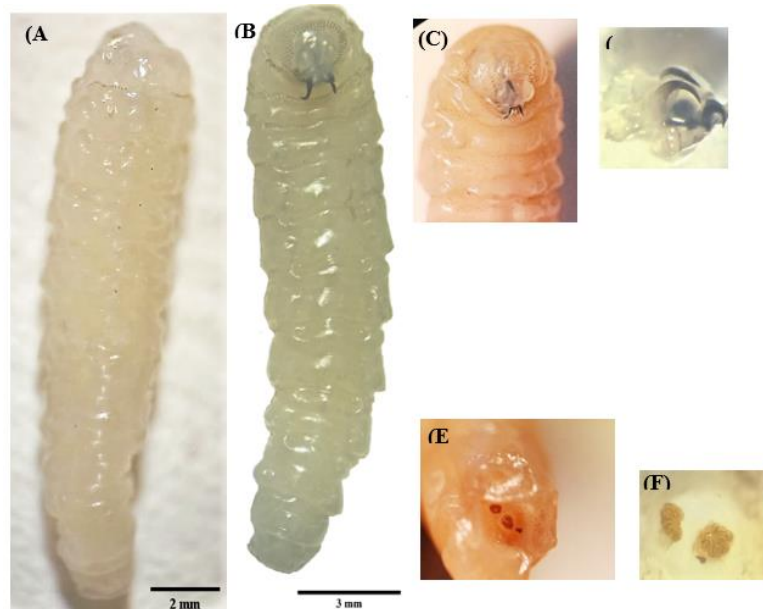


Fig. 6: Light microscope images of *Cephalopina titillator* second instar larvae. (A) (dorsal) & (B) (ventral) habitus of the whole-body structure. (C) The antero-ventral part of the body with the pseudocephalon bears the antennal lobes and the mouth hooks complex structure, (D) fusion of the mandible and maxillae of the mouth parts structures (E) The posterior part of the body showing the spiracular preitremes, (F) the falciform spiracular openings.

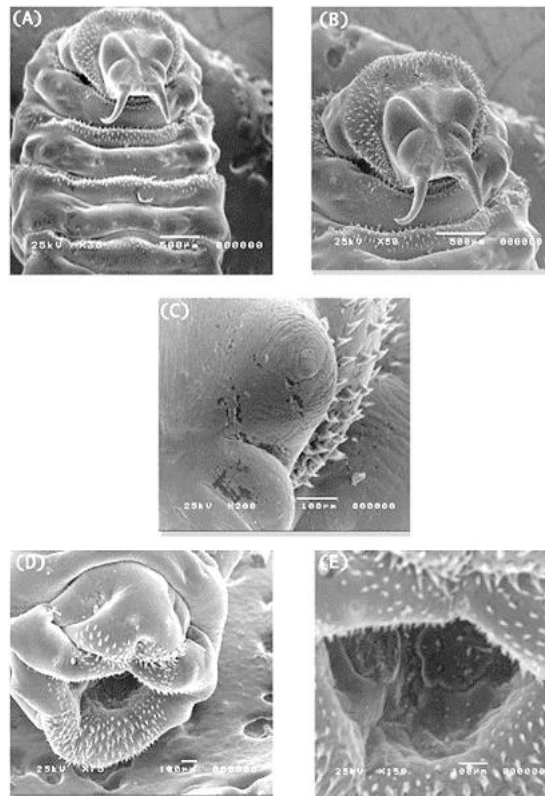


Fig. 7: Scanning electron micrograph of the 2nd larval instar of *Cephalopina titillator*. (A) Body spinulation and the intersegmental grooves, (B) The unarmed pseudocephalum and 1st thoracic segment, (C) antennal lobes, (D) last abdominal segment showing upper and lower lips surround the spiracle and (E) posterior spiracular plates sunken in a groove.

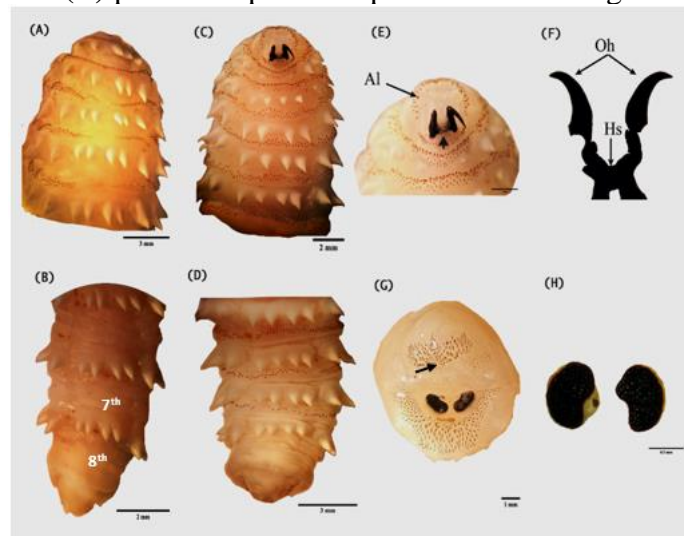


Fig. 8: Light microscope images of *Cephalopina titillator* third stage larvae showing the main morphological characteristics. (A) antero-dorsal part with incomplete rings of spines. (B) postero-dorsal part with 7th and 8th segments with no spines, (C) spinulation of antero-ventral part, (D) postero-ventral part with a gradual decrease in spinulation and lack of spines on the last abdominal segment. (E) Magnification of the pseudocephalum showing the atrium (Arrowhead) and antennal lobes (Al). (F) Cephalopharyngeal skeleton (Oh: oral hooks; Hs: hypostomal sclerite). (G) The terminal end (lips) of the last abdominal segment shows the spiracular peritremes and the anal orifice (Arrow) on the anal papillae. (H) Posterior spiracles with numerous oval-to-kidney shaped spiracular pores.

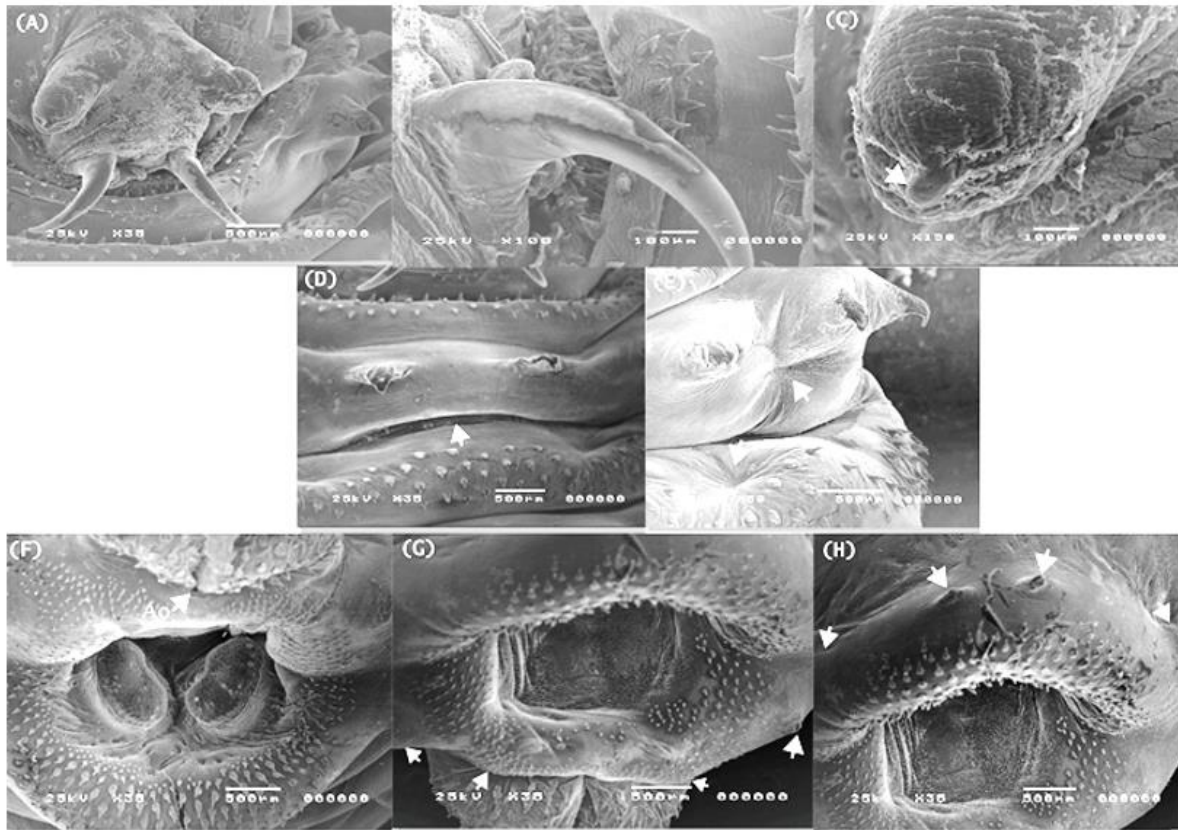


Fig. 9: Scanning electron micrograph of the 3rd stage larvae *Cephalopina titillator*. (A) Magnification of the pseudocephalon region. (B) Maxillae (C) Antennal lobe with pseudocelli (Arrow), (D) Ventral view of the thoracic region with the cuticular groove. (E) cuticular pits on the 2nd and 3rd thoracic region. (F) Lips on the last abdominal segment shows the spiracular peritremes and the anal orifice (AO) on the anal papillae. (G) 4 tubercles (Arrows) on lower lip. (H) 4 tubercles (Arrows) on upper lip.

Examination of the *C. titillator* Adult Flies:

Adults *C. titillator* are medium in size, with a mean body length of 9.56 ± 0.3 mm for females and 8.55 ± 0.67 mm for males. The body composition follows the general structure of the calyprate flies (Fig.10 A-C, Fig.11 A &B). The adult head is oval to rounded in shape, orange at the apex, and pale yellow in the lower part; eyes are widely separated in males (Fig.10D), narrowly separated in the females, with the para-frontal region approximately $\frac{1}{2}$ of the length in case of male (Fig.11D). Eyes are mediated by the antennal groove in which antenna was separated by heart-shaped median ptilinum fissures. In the upper part of the head, the ocellar triangle is darkened and contained three black rounded spots

surrounded by sensory hairs in both sexes (Fig.11E, Fig.12C).

The antennal structure of *C. titillator* is characterized by its segmental structure, proximal scape cap-like; antennal pedicel triangular in shape; flagellum relatively globular, with a cylindrical arista bearing tiny sensory sensilla (Fig.12A&B). The rudimentary mouth parts are represented by only the epistome, which comprises three segments, two ovals laterally separated by a long median one, which is wider in females than in males (Fig.10E, Fig.11F).

Prescutum in males (Fig.10A) with three large black patches the middle one is surrounded by white borders on the lateral and basal sides; scutum with a middle sub-quadrangle gray patch at lower margin, and 5-6 sub-basal small gray to black patches;

prescutum in female (Fig.11A) with seven black patches, three sub-marginal and two at middle; scutum with a middle complex brown patch surrounded by two longitudinal ones. Scutellum with face-like ornamentation in both sexes, moreover the scutellum structure in females is wider than in males. Legs brown in colour, with black banding on femur, tibia and tarsi; tibia with two apical spurs, tarsi 5 segmented, 1st segment the longest, the 4th segment the shortest, 2nd to 4th segments heart-shaped (Fig.10G&H) and the last tarsal segment ended with two curved claws and two pad-like pulvilli (Fig.12D).

Wings are clearly transparent

without any markings or spots, covered with small spines, especially around the veins. The radius vein (R4+5) meets the median (M1) at two points, in middle at the anterior cross vein (r + m) forming a closed cell (1st basal cell) with condensed hairs at their meeting point, at the apex forming an apical cell, blunt notched shape in male (Fig.10F), sharply evaginated in female (Fig.11C). Abdomen (Fig.10B, Fig.11B) creamy-white in colour, with scattered dark brown-to-black spots in upper and lateral sides. In males, the external genital structures are bulging (Fig. 10B) while in females they form a sunken triangle (Fig.12E).

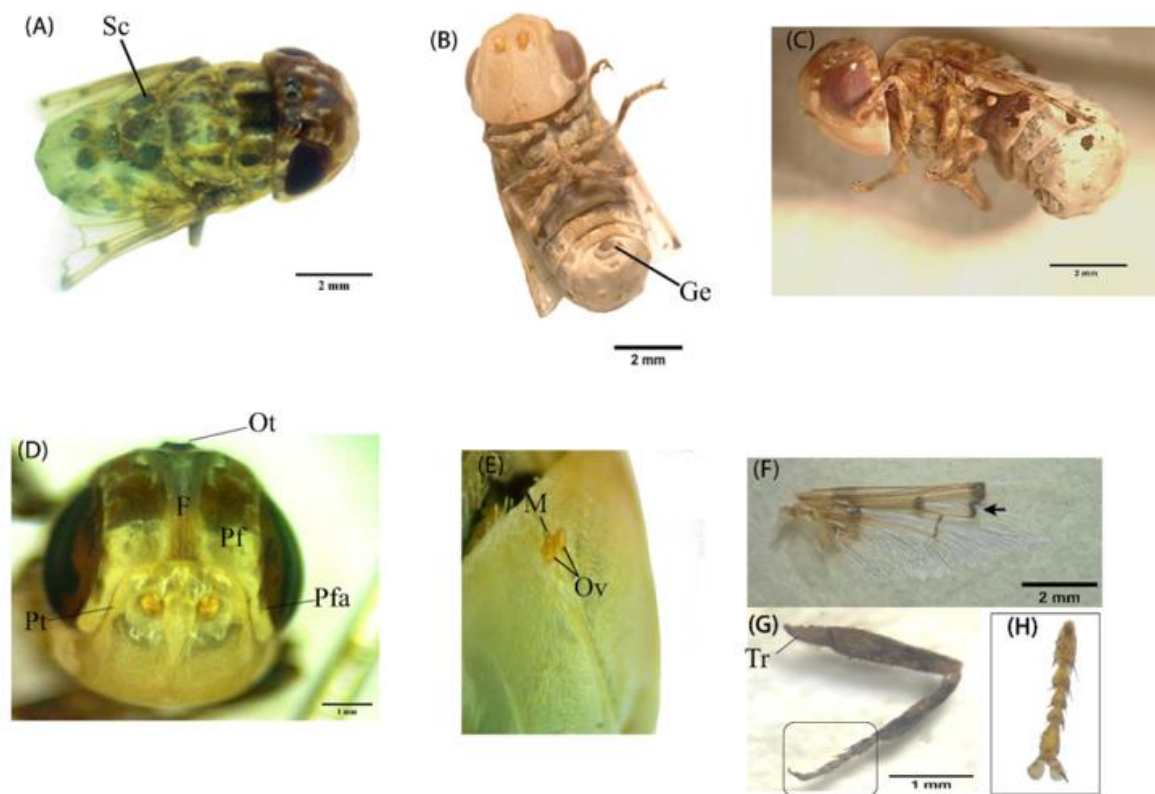


Fig.10: Light microscope images of the male adult stages of *Cephalopina titillator*. (A) Dorsal view of habitus showing special ornamentation around compound eyes, scutellum (Sc) and abdomen. (B) Ventral view of habitus showing the bulging genitalia (Ge) characteristic to males. (C) Left lateral view of habitus (D) Frontal view of the head region showing ocular triangle (Ot) with black ocelli, parafrenal (Pf) region, parafacial (Pfa) region, ptilinum (Pt). (E) Magnification of the epistome with 2 oval segments (Ov) separated by a median (M) protrusion. (F) Wing showing the male-characteristic blunt notched shape (black arrow) of the cross wing (r+m). (G) foreleg with the banding coloration and the emerging spines on the different parts, (H) Magnification of the tarsal region.

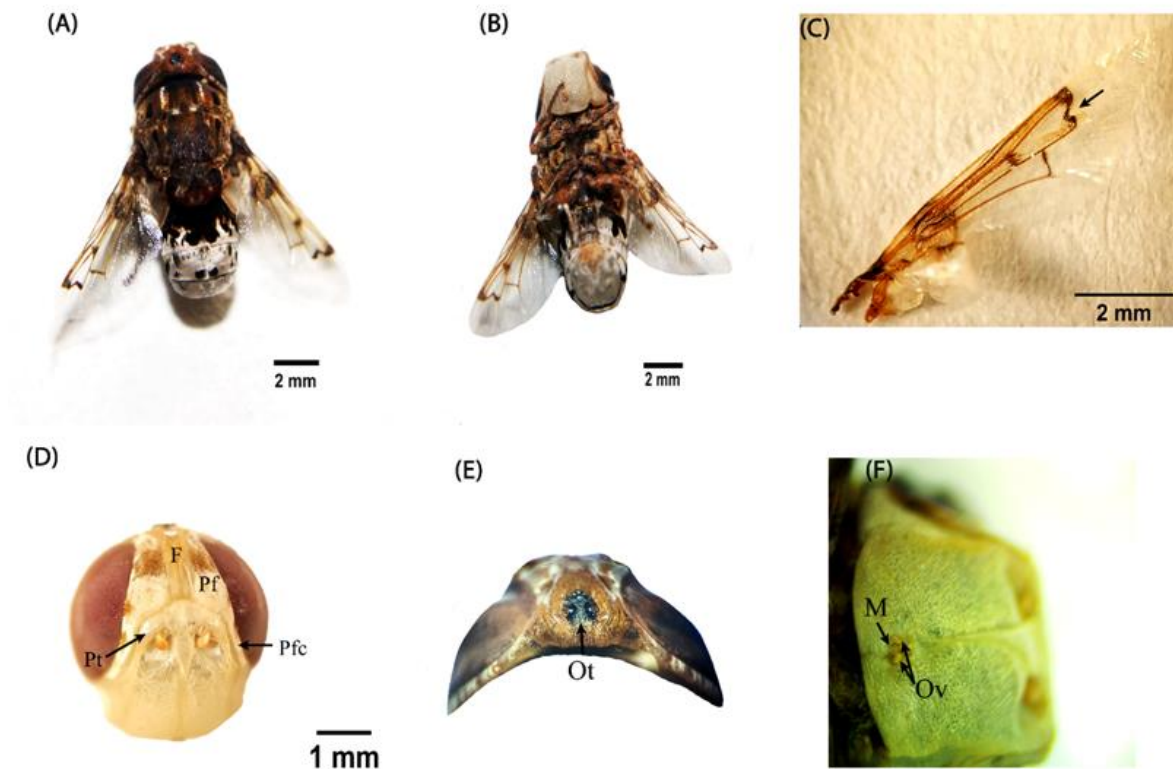


Fig. 11: Light microscope images of the female adult stages of *Cephalopina titillator*. **(A)** Dorsal view of the habitus showing the general body structure **(B)** Ventral view of habitus. **(C)** Wing structure with the female-characteristic sharp evagination of the cross wing (r+m). **(D)** Frontal view of the head region with the larger compound eyes and narrower parafrontal (Pf) and parafacial (Pfc) region. **(E)** Magnification of the upper head region showing the triangular ocelli (Ot) accompanied with sensory hairs. **(F)** Magnification of the epistome showing the 2 oval segments (Ov) and a median (M) protrusion which appear to be shorter than that of the male.

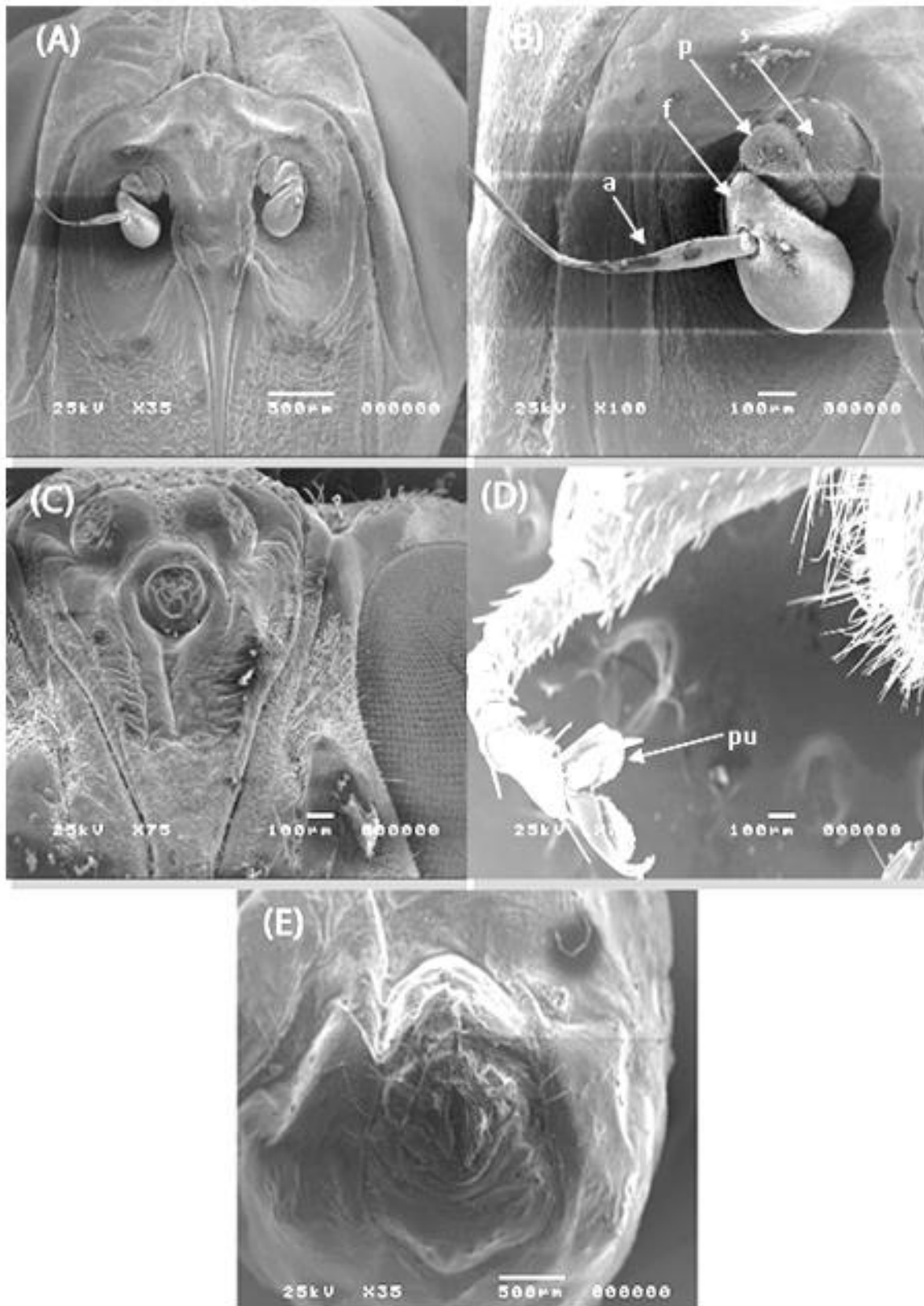


Fig. 12: Scanning electron micrograph of the female adult stage *Cephalopina titillator*. **(A)** Magnification of the facial region showing the pair of antennae. **(B)** Magnification of the antennae showing the 3 typical parts: scape(s), pedicel(p) and flagellum (f) with the arista (a) **(C)** triangular ocellar region bearing 3 ocelli surrounded by the sensory hairs, **(D)** tibial & tarsal segments of the foreleg ending with a pair of claws and pulvelli (pu). **(E)** genital opening.

DISCUSSION

Due to the great attention given by the Egyptian government to the camels as an animal industry and as an additional source of animal protein besides its value as working animals. This study focused on studying the ecological and morphological aspects of one of the important endoparasites infesting camels and causing an economic loss, the nasal bot fly, *C. titillator*.

The present study reveals a strong negative correlation between the rate of larval infestation per animal in relation to the ambient temperature ($r = -0.85$, $P = 0.00046$). The total infestation rate was 53.23% throughout a year of sampling. This result is relatively comparable with that obtained by Khater *et al.* (2013) who showed that the prevalence of *C. titillator* larvae in Egypt was 41.67%. However, other Egyptian studies reported a lower incidence of infestation rate with 25% (Morsy *et al.*, 1998).

In comparison *C. titillator* larvae infestation rates of camels in the neighbouring countries, our results in the current study are close to the recorded infestation rates of 52% (Fatani and Hilali 1994) and 41% (Alahmed 2002) in Saudi Arabia. In Jordan Al-Ani and Amr (2016) reported 46% and in Iraq Al-Jindeel *et al.* (2018) reported 40.07%, while in Iran, Jalali *et al.* (2016) reported an infestation rate of 52.3%. Higher incidence rates were recorded in different countries: 91.4% in Saudi Arabia (Hussein *et al.* 1982), 69.9% in Nigeria (Desbordes and Ajogi 1993), 71.7% in Ethiopia (Bekele 2001), 58.1% in Iran (Oryan *et al.*, 2008), 79% in Libya (Abd El-Rahman 2010), 80.72% in Iran (Shakerian *et al.*, 2011), 82.6% in Ethiopia (Kissi and Assen 2018), and even reached the extreme being 100% in Sudan (Musa *et al.*, 1989).

The observed variations in the rate of infestation rates in different countries might be attributed to the botfly larval populations involved, the number of

inspected animals and rearing conditions, study localities and the prevailing environmental conditions.

Regarding the monthly prevalence of *C. titillator* larvae among camels, the percentage of infestation reached the peak from November 2019 to February 2020 with a percentage of 80%, with a gradual decrease to 60% in January 2020. Moreover, a steady decrease was noticed until the end of the collection period when it reached 40% in May 2020. The infestation rate was 20% in July 2019.

There were differences between the monthly highest and lowest infestation incidences, not only between the different countries but also between the same county in different years. In Egypt, Morsy *et al.* (1998) observed that the highest prevalence periods were in October, 25%, without any record of the climatic conditions during the study. In Saudi Arabia, Fatani and Hilali (1994) observed that the highest prevalence was reached in two peaks, 94.06% in February and 88.90% in September, while the lowest prevalence 1.43% was in June however, Alahmed (2002) found that where the highest peak was recorded in April reaching 99% while in July the lowest infestation rate recorded with 4%. In Jordan, Al-Ani and Amr (2016) noticed that the highest (87.5%) and the lowest (17.64%) percentages were in January and May, respectively. In Iraq, Al-Jindeel *et al.* (2018) found that the highest infestation rate was in January with 89.02% and the lowest was in July with 6.15%. In Nigeria, Desbordes and Ajogi (1993), recorded the monthly prevalence of *C. titillator* larvae in slaughtered camels reaching the highest rate of prevalence (91.4%) in September, while the lowest rate of prevalence (47.4%) was in May.

The seasonal prevalence and the larval index (number of larvae per infested animal) were observed. In the winter season, the seasonal prevalence reached its maximum with 73.3% where the larval index reached (15.54), especially in

December 2019 with (16.5). Both the prevalence and larval index decreased during the autumn and spring seasons, with 60% (13.3) and 53.3% (11.25), respectively. It reached its lowest value during summer with 29.41% (9.6), especially in June at 28.6% (9.5). These results consolidate the larval flourishing when the temperature decreases.

Nevertheless, Morsy *et al.* (1998) stated that the autumn season was with the highest prevalence with 25.7% in Egypt. Our result was supported by Oryan *et al.* (2008) in Iran where they found that the prevalence was greater in the colder months (69.8%) compared to those of warmer ones) and 36.2%. In addition, Jalali *et al.* (2016) found that the infestation rate was significantly higher in colder months (62.5%) compared to warmer ones) and 32% in Iran. Al-Ani and Amr (2016) also noticed that the highest number of infested camels was during the cold months (November, 33.3% to March, 75%) then declined in the summer and raised again in late summer (August, 57.14%) in Jordan. The reason for this low prevalence in warm seasons might be due to the small size of the first instar larvae that cannot be reached in most cases (Fatani and Hilali 1994).

A collection of both the second and third larvae of *C. titillator* revealed that the third instar predominated over the second instars. The total number of the third instars during the collection period reached 310 larvae with approximately 9.39 larvae per infected animal with a percentage of 72.26% of total larvae collected. The second stage reached 119 larvae with approximately 3.60 larvae per infected animal with a percentage of 27.74% of total larvae collected. This population bias towards the domination of the third instars over the second instars might be owed to the longer developmental period for the third instars to reach full maturity before leaving the host body. (Morsy *et al.*, 1998). In Jordan, the same conclusion was reached, where they obtained a total number of third and second instars of 469 and 37 for the

same time period, respectively, with the percentage of the third instars (90.7%) substantially higher than that of the second instars (7.16%) (Al-Ani and Amr, 2016). While in Saudi Arabia, Alahmed (2002), reported different results, where the second instar numbers slightly surpassed the third instar. He collected 591-second instar larvae (35%) with ~1.68 larvae per infected animal, compared to 577 third instar larvae (35%) with approximately ~1.64 larvae per infected animal.

The morphological studies and description of the external features of both sexes for the adult stage and larval stage of *C. titillator* larval instars revealed a tiny size of 0.7 mm in the 1st instars according to Zumpt (1965). Further, the results showed that most of the morphological features of the 2nd and 3rd larval instars including body pseudocephalon, spinulation and the structure of the spiracles are comparable to those reported in other studies (Guitton *et al.*, 1997, El-Bassiony and Awad, 2007, Attia and Mahdy, 2021). The presence of the mandibles under the cuticle of the 2nd instars is reported in this study for the first time, a result that is similar in other fly species, the horse botfly, *Gasterophilus intestinalis* (Abdel Rahman *et al.*, 2018). The 3rd instar spine pattern and the presence of the fleshy spines are unique features in *C. titillator*. Moreover, the terminus lips enclose a characteristic feature, a pair of irregularly pored spiracular peritremes, which might be used for accurate identification of the 3rd instars. In spite of many studies available, there is still an apparent difficulty in differentiating the larval instars (Al-Jindeel *et al.*, 2018), Toaleb and Abdel-Rahman, 2021). Therefore, the results obtained in the current studies on body size, presence of fleshy processes, shape and opening size of spiracles, together with measurements reported in other studies can be collated and integrated to construct a key for easy and accurate differentiation between the 2nd and third larval instars of *C. titillator*.

Concerning the adult stages, the emergence process occurred in the early morning of the day, which may indicate the effect of temperature, humidity, and photoperiod as environmental factors affecting the emergence of these flies.

Detailed morphological features of both sexes of *C. titillator* are introduced in the current investigation and showed that Body size, eye shape, the width of the prefrontal region, width of a median segment of epistome, shape of the outer cell formed by meeting radius vein (R4+5) with the median (M1), the width of scutellum, and genital opening shape are considered as important key features for sex differentiation. As it is well known that most oestrids have rudimentary mouth parts, *C. titillator* is considered one of the ideal examples exhibiting this feature (Wood 2006). The owl face-like ornamentation on scutellum in both sexes may be a mimic feature for this short-aged fly. Body size, eye shape, the width of the prefrontal region, width of the median segment of epistome, shape of the outer cell formed by meeting radius vein (R4+5) with the median (M1), the width of scutellum, and genital opening shape are considered as important key features for sex differentiation.

Conclusion

This study shed the light on the different stages of *C. titillator* with a great focus on some ecological and morphological aspects to reveal the secretive life cycle of this species in relation to their hosts. The detailed description of the body structures will aid in the appropriate identification and classification. Additional molecular and phylogenetic work is needed to establish the evolutionary relationships among the oestrid group of insects with specialized habits and habitats.

Ethical Approval: This research paper was approved by the research ethics committee from Faculty of Science, Ain Shams University (ASU-SCI/ENTO/2022/10/6).

REFERENCES

- Abd El-Rahman, S. (2010). Prevalence and pathology of nasal myiasis in camels slaughtered in El-Zawia Province-Western Libya: with a reference to thyroid alteration and renal lipidosis. *Global Veterinaria*, 4:190–197.
- Abdel Rahman, M.M., Hassanen, E.A., and Abdel Mageed, M.A. (2018). Light and scanning electron microscopy of *Gasterophilus intestinalis* (larvae and adult fly) infesting donkeys with emphasis on histopathology of the induced lesions. *Egyptian Veterinary Medical Society of Parasitology Journal*, 14(1): 15-31.
- Alahmed, A.M.I. (2002). Seasonal Prevalence of *Cephalopina titillator* Larvae in Camels in Riyadh Region, Saudi. *Arab Gulf Journal of Scientific Research*. 20(3): 161-164.
- Al-Ani, F., and Amr, Z. (2016). Seasonal prevalence of the larvae of the nasal fly (*Cephalopina titillator*) in camels in Jordan. *Revue d'élevage et de médecinevétérinaire des pays tropicaux*, 69(3): 125-127.
- Al-Jindeel, T.J., Jasim, H.J., Alsalih, N.J., and Al-Yasari A.M.R. (2018). Clinical, immunological and epidemiological studies of nasopharyngeal myiasis in camels slaughtered in Al-Muthanna province. *Advances in Animal and Veterinary Sciences*, 6(7): 299-305.
- Angulo-Valadez, C.E., Scholl, P. J., Cepeda-Palacios, R., Jacquet, P., and Dorchies, P. (2010). Nasal bots... a fascinating world! *Veterinary Parasitology*, 174(1-2): 19-25.
- Attia, M.M., and Mahdy, O.A. (2021). Fine structure of different stages of camel nasal bot; *Cephalopina*

- titillator* (Diptera: Oestridae). *International Journal of Tropical Insect Science*, 1-8.
- Bekele, T. (2001). Studies on *Cephalopina titillator*, the Cause of Sengale in Camels (*Camelus dromedarius*) in Semi-arid Areas of Somali State, Ethiopia. *Tropical Animal Health and Production*, 33(6): 489-500.
- Colwell, D.D. (1986). Cuticular sensilla on newly hatched larvae of *Cuterebrafontinella* Clark (Diptera: Cuterebridae) and *Hypoderma* spp. (Diptera: Oestridae). *International Journal of Insect Morphology and Embryology*, 15(5-6): 385-392.
- Colwell, D.D. (2006). Life cycle strategies. The Oestrid Flies: Biology, Host-Parasite Relationships, Impact and Management. Cambridge: CABI Publishing. 67-77.
- Desbordes, O.K., and Ajogi, I. (1993). Seasonal prevalence of *Cephalopina titillator* myiasis in camels (*Camelus dromedarius*) in Sokoto State, Nigeria. *Veterinary Parasitology*, 50(1-2): 161-164.
- El Bassiony, G.M., and Awad, H.H. (2007). Surface ultrastructure of the third-instar larva of *Cephalopina titillator* (Diptera: Oestridae). *Journal-Egyptian German Society of Zoology*, 52(E): 20.
- El-Bassiony, G.M., Al-Sagair, O.A., El-Daly, E.S., and El-Nady, A.M. (2005). Alterations in the pituitary-Thyroid axis in camel *Camelus dromedarius* infected by larvae of nasal bot fly *Cephalopina titillator*. *Journal of Animal and Veterinary Advances*, 4(3):345-348.
- Fahmy, M.M., Ashmawy, K., and Omar, H.M. (1985). Studies on the nasal botfly of camel, *Cephalopina titillator*. *Journal of the Egyptian Veterinary Medical Association*, 45: 311-317.
- Fatani, A., and Hilali, M. (1994). Prevalence and monthly variations of the second and third instars of *Cephalopina titillator* (Diptera: Oestridae) infesting camels (*Camelus dromedarius*) in the Eastern Province of Saudi Arabia. *Veterinary Parasitology*, 53(1-2), 145-151.
- Guitton, C., Dorchie, P., and Morand, S. (1997). Morphological comparison of second stage larvae of *Oestrus ovis* (Linnaeus, 1758), *Cephalopina titillator* (Clark, 1816) and *Rhinoestrus usbekistanicus* Gan, 1947 (Oestridae) using scanning electron microscopy. *Parasite*, 4(3): 277-282.
- Hartvigsen, G. (2014). A primer in biological data analysis and visualization using R. In A Primer in Biological Data Analysis and Visualization Using R. Columbia University Press. ISBN: 9780231166997.
- Hussein, M.F., Elamin, F.M., El-Taib, N.T., and Basmaeil, S.M. (1982). The pathology of nasopharyngeal myiasis in Saudi Arabian camels (*Camelus dromedarius*). *Veterinary Parasitology*, 9(3-4): 179-183.
- Hilali, M.A., Mahdy, O.A., and Attia, M.M. (2015). Monthly variations of *Rhinoestrus* spp. (Diptera: Oestridae) larvae infesting donkeys in Egypt: Morphological and molecular identification of third stage larvae. *Journal of Advanced Research*, 6(6): 1015-1021.
- Jalali, M.H.R., Dehghan, S., Haji, A., and Ebrahimi, M. (2016). Myiasis caused by *Cephalopina titillator* (Diptera: Oestridae) in camels (*Camelus dromedarius*) of semi-arid areas in Iran: distribution and

- associated risk factors. *Comparative Clinical Pathology*, 25(4): 677-680.
- Kamal, M., Yasmeen, G., Naz, F., Saher, N.U., Ahmad, N., Khan, W., and Yousafzai, G. J. (2021). Morphotaxonomy and allometry of *Oestrus ovis* (LINNÉ, 1758) larvae (Diptera: Oestridae: Oestrinae). *Journal of Animal and Plant Sciences*, 31(2).
- Khater, H.F., Mohamed, Y.R., and Abla, D.A. (2013). *In vitro* control of the camel nasal botfly, *Cephalopina titillator*, with doramectin, lavender, camphor, and onion oils. *Parasitology Research*, 112(7): 2503-2510.
- Kissi, L.M., and Assen, A.M. (2018). Prevalence, Larvae Burden and Gross Pathological Lesion of *Cephalopina titillator* in Camels Slaughtered at Addis Ababa Abattoir Akaki Branch, Ethiopia. *Journal of Veterinary Science and Technology*, 8(6): 1-5.
- Li, X.Y., Chen, Y.O., Wang, Q.K., Li, K., Pape, T., and Zhang, D. (2018). Molecular and morphological characterization of third instar Palaearctic horse stomach bot fly larvae (Oestridae: Gasterophilinae, Gasterophilus). *Veterinary Parasitology*, 262:56-74.
- Li, X.Y., Yan, L.P., Pape, T., Gao, Y.Y., and Zhang, D. (2020). Evolutionary insights into bot flies (Insecta: Diptera: Oestridae) from comparative analysis of the mitochondrial genomes. *International Journal of Biological Macromolecules*, 149: 371-380.
- Locklear, T.R., Videla, R., Breuer, R.M., Mulon, P.Y., Passmore, M., Mochel, J.P and Smith, J.S. (2021). Presentation, Clinical Pathology Abnormalities, and Identification of Gastrointestinal Parasites in Camels (*Camelus bactrianus* and *Camelus dromedarius*) Presenting to Two North American Veterinary Teaching Hospitals. A Retrospective Study: 1980–2020. *Frontiers in Veterinary Science*. 1- 8. <https://doi.org/10.3389/fvets.2021.651672>
- Mahdy, O.A., and Attia, M.M. (2021). Comparative micro-morphological and phylogenetic analysis between *Rhinoestrus purpureus* and *Rhinoestrus bekistanicus* (Diptera: Oestridae) larvae and its adults. *International Journal of Tropical Insect Science*, 41(1): 241-250.
- Morsy, T.A., Aziz, A.S., Mazyad, S.A., and Al Sharif, K. (1998). Myiasis caused by *Cephalopina titillator* (Clark) in slaughtered camels in Al Arish Abattoir, North Sinai governorate, Egypt. *Journal of the Egyptian Society of Parasitology*, 28(1): 67-73.
- Musa, M. T., Harrison, M., Ibrahim, A.M., and Taha, T.O. (1989). Observations on Sudanese camel nasal myiasis caused by the larvae of *Cephalopina titillator*. *Revue d'élevage et de médecinevétérinaire des pays tropicaux*, 42(1): 27-31.
- Negm-Eldin, M.M., Elmadawy, R.S., and Hanan, G.M. (2015). *Oestrus ovis* larval infestation among sheep and goats of Green Mountain areas in Libya. *Journal of Advanced Veterinary Animal Research*, 2(4): 382-387.
- Otranto, D. (2001). The immunology of myiasis: parasite survival and host defense strategies. *Trends in Parasitology*, 17(4): 176-182.
- Oryan, A., Valinezhad, A., and Moraveji, M. (2008). Prevalence and pathology of camel nasal myiasis in eastern areas of Iran. *Tropical*

- Biomedicine*, 25(1): 30-36.
- Ruiz-Martines, I., and Palomares, F. (1993). Occurrence and overlapping of pharyngeal bot flies *Pharyngo myiapicta* and *Cephenemyia auribarbis* (Oestridae) in red deer of southern Spain. *Veterinary Parasitology*, 47: 119-127.
- Shakerian, A., Hosseini, S.R., and Abbasi, M. (2011). Prevalence of *Cephalopina titillator* (Diptera: Oestridae) larvae in one-humped camel (*Camelus dromedarius*) in Najaf-Abad, Iran. *Global Veterinaria*, 6(3): 320-323.
- Schauff, M. E. (Ed.). (2001). Collecting and preserving insects and mites: techniques and tools. *Systematic Entomology Laboratory, USDA, National Museum of Natural History, NHB 168, Washington, D.C. 20560*.
- Schneider, C.A., Rasband, W.S., and Eliceiri, K.W. (2012). NIH Image to ImageJ: 25 years of image analysis. *Nature Methods*, 9(7): 671-675.
- Toaleb, N.I., and Abdel-Rahman, E.H. (2021). Accurate diagnosis of camel nasal myiasis using specific second instar larval fraction of *Cephalopina titillator* extract. *Advances in Animal and Veterinary Sciences*, 9(5): 674-681.
- Wood, D.M. (2006). Morphology of Adult Oestridae In: Colwell DD, Hall MJR, Scholl PJ, editors. *The oestrid flies: biology, host-parasite relationships, impact and management*. Wallingford: CABI. 79-80.
- Zumpt, F. (1965). Myiasis in man and animals in the old world. A textbook for physicians, veterinarians and zoologists. *Butterworths, London, United Kingdom*

ARABIC SUMMARY

التوزيع الموسمي والتوصيف المورفولوجي لذبابة نغف الجمل سيفالوبينا تيتيلاتور (ثنائيات الاجنحة: عائلة النبريات) المجمعة من المجازر في مصر

شريف حامد، مني جابر شعلان، عماد ابراهيم خاطر، محمد امين قناوي، ايناس حمدي غلاب
قسم علم الحشرات-كلية العلوم-جامعة عين شمس

تعتبر الإبل العربية (*Camelus dromedarius*) من أهم أنواع الماشية التي لها تأثير كبير على حياة الإنسان خاصة اقتصادياً. تأتي مرحلة اليرقات لذبابة نغف الجمل الأنفية، (*Cephalopina titillator* (Diptera: Oestridae)، علي رأس قائمه اهم الطفيليات الداخلية اجباريه التطفل و التي تسبب التئويد البلعومي الأنفي مما يؤدي إلى خسارة اقتصادية و ثقافيه لانتاج الإبل في جميع أنحاء العالم. فعلى الرغم من أن الطور البالغ للذبابة ليس متطفلاً، وغير قادر على التغذية، فإن بقاءه على قيد الحياة موقوف على مخزونه الغذائي من مرحلة اليرقات. في مصر، لا يُعرف سوى القليل عن العوامل البيولوجيا والبيئة لذبابة *C. titillator* ودور العوامل البيئية المحيطة في التأثير على نمو اليرقات المرتبطة بالإبل كعائل لها تحت ظروف المختبر فقط. لمعالجة هذه الفجوة المعرفية، قمنا بدراسة الشكل الظاهري والتركيب المجتمعي والانتشار الموسمي للمراحل اليرقات لذبابة *C. titillator* في الجمال في مصر. تم تجميع 429 يرقة من الطور اليرقي الثاني والثالث من رؤوس الإبل المذبوحة في مجزر البساتين على مدار 12 شهر بدايه من يونيو 2019 وحتى مايو 2020. فكانت نسبة الاصابه باليرقات المتطفله من بين 62 رأس حيوان تم فحصها، 33 مصابون بنسبه (53.23%). تم تربيته يرقات الطور الثالث في المختبر في درجات حرارة محببة مختلفة وملاحظتها حتى خروج الاطوار البالغة. تم تقديم توصيف مورفولوجي وبنية دقيقه مفصل لكل من اطوار اليرقات والذبابة البالغ باستخدام كلا من المجهر الضوئي والمجهر الماسح الإلكتروني، على التوالي. هذه الدراسة أكدت اهميه خصائص الجسم واهم السمات المورفولوجيه التي تفرق ما بين الجنسين في الذباب البالغ.